Kresling Magnetic Soft Robotics

THESIS

Presented in Partial Fulfillment of the Requirements for the Degree Master of Science in the Graduate School of The Ohio State University

By

Yue Sun

Graduate Program in Mechanical Engineering

The Ohio State University

2021

Dissertation Committee:

Ruike, Zhao, Ph. D., Advisor

Soheil, Soghrati, Ph. D., Committee Member

Abstract

Due to a greater variety of applications required for robotics, soft robotics has been studied because of its untethered control, fast transformation, and biocompatibility. Soft magnetic material was developed by embedding hard magnets into a silicone-based soft matrix. Once programmed, the material provides magnetic torque remotely. However, with the simple geometry and structural design of the magnetic soft material, the system is always limited to simple deformations, such as bending and folding. To improve the capability of the system, origami structures were incorporated into the magnetic material in our current work. By putting magnetically programmed materials on the origami structures, the deformation of the system can be controlled using three-dimensional magnetic fields. The system can, therefore, achieve multiple deformation modes, such as elongation, bending, and sequential folding. Our experimental results are proof of this concept. For Kresling origami structures, the heights vary based on the torque generated by the magnetic fields. By switching the materials used and the designs of the creases, the properties can be changed and controlled. Different types of structures can be used for robotics in various applications. This study can be used in many applications, such as the composition of a soft robotic system.

Acknowledgments

I would like to express my sincerest gratitude to many faculties and friends that have supported and encouraged me throughout my studies at the Ohio State University. I cannot succeed without them. Special thanks to Dr. Ruike Zhao for having me in her research lab. I have gained a profound understanding of the process of research, and this experience is beneficial for my lifetime.

I am very much thankful to Dr. Soghrati for his valuable time as a member of my committee. I thank all the members profusely in the SIM Lab for their patience and kindness.

Finally, I would like to appreciate all the people who have not been mentioned but inspired me greatly.

Vita

Education

The Ohio State University, Columbus, OH Aug. 2018–Present

- Anticipate graduating in May 2021 with B.S. in Mechanical Engineering and Mathematics Minor
- Honors in Undergraduate Research Distinction

Tacoma Community College, Tacoma, WA Sept. 2016–May 2018

- Associates of Science Degree, Associates of Art and Science Degrees
- First student graduate with Honor's Distinction Pathway
- Member of Phi Theta Kappa

Whatcom Community College, Bellingham, WA Sept. 2015–June 2016

- Non-degree Study

Publications

Qiji Ze, Shuai Wu, Larissa S. Novelino, Jun Nishikawa, Jize Dai, Yue Sun, Glaucio H. Paulino, Ruike Zhao. Transformer Origami Robots for Targeted Drug Delivery (submitted)

Fields of Study

Major Field: Mechanical Engineering

Table of Contents

List of Figures

Introduction

The use of robotics has many applications due to the fast development of technology. Different forms of robotics are used to achieve various goals. Rigid robotics are most common in today's world. Many limitations have showcased its disadvantages in some fields, such as the medical and bio-medical fields. Due to the complexity of human body, robots generally cannot reach some areas to complete operations.

Figure 1. Da Vinci Robot during an Operation (1)

The limitations of rigid robots have inspired the development of soft robotics. For example, Figure 1 shows a robot called Da Vinci, created by Intuitive Surgical. It has four arms to assist surgeons. If the rigid arms are replaced with soft materials, then the number of robotics arms can be decreased to make procedures easier under proper

control.

Background

Compared to traditional robotics characterized by rigid, actuated, and programmed mechanical components, recent advances in soft robotics have showcased a new generation of engineering devices and systems with unprecedented functionalities and superior machine–human interactions (2–5). Among the various elements of soft robotics, a critical element is utilizing stimuli-responsive materials paired with advanced geometric designs to achieve more complex behavior and versatile functions compared to conventional robots. In particular, magnetically-responsive soft materials have gained significant attention in the fields of engineering and medicine due to the efficiency of manipulation, adaptability to the surrounding environment, and ease of remote actuation that then enable under the applied magnetic field (6–8).

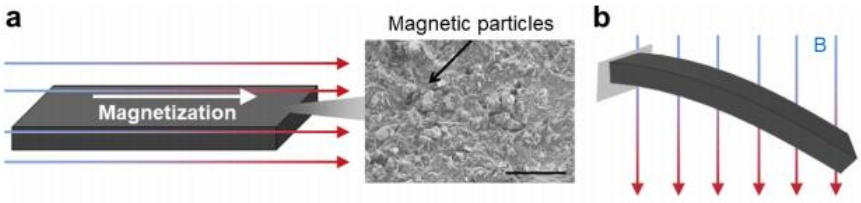

Figure 2. Hard-magnetic soft material and the multimodal deformation mechanism. (8) (a) Schematics of a hard-magnetic soft material. The scale bar in the missile image is 30 μm. (b) Actuation of the hard-magnetic soft material.

The previous figure presents the deformations of hard-magnet soft material under different magnetic fields. Soft robotics can be produced using magnetic materials. Figure 3 shows several recent examples of magnetic soft robots with unique functions

and performance.

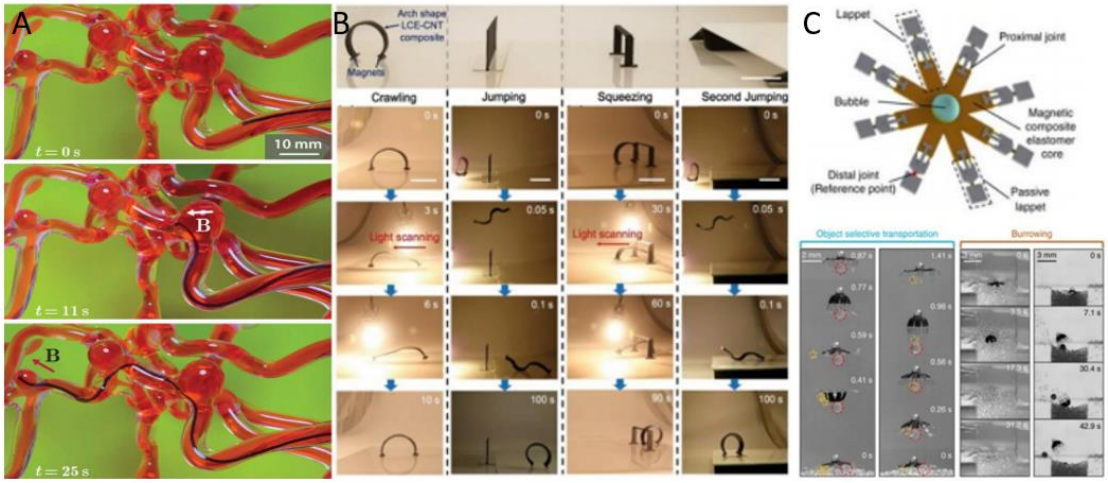

Figure 3. Recent examples of magnetic soft robotics. (A) soft continuum robot passing through a 3D cerebrovascular phantom network (9); (B) Multimodal locomotion of the soft robot made of elastomer-carbon nanotube composite powered by light (10); (C) A jellyfish-like robot design and four different tasks realized by the jellyfish-like untethered magnetic soft swimmer robot (10).

Compared to traditional rigid robotics, magnetic soft robotics has the advantages of untethered control, fast transformation, broad scale range, and biocompatibility. Although the magnetic itself can be controlled and deformed by changing the strength of the magnetic field applied, the structure can be deformed if it is incorporated with origami structures. *Origami* is a Japanese word that means “paper folding.” The structures are examined under folded and deployed states. When a magnetic disk is attached to an origami structure, the structure can be actuated and, therefore, deformed under different magnetic fields.

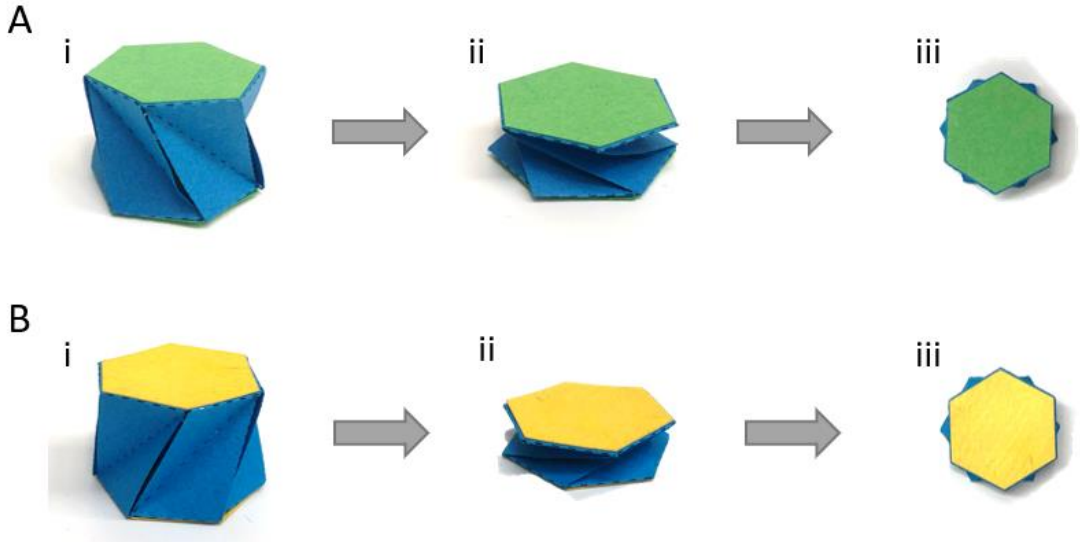

Figure 4. Kresling origami structures with opposite directions. (A) Clockwise folding Kresling structure: (i) deployed stable state; (ii) folded stable state; (iii) folded state top view. (B) Counterclockwise folding Kresling structure: (i) deployed stable state; (ii) folded stable state; (iii) folded state top view.

One of the advantages of Kresling structures is that they can provide an up and down motion of the magnetic disk when a torsional magnetic field is applied. Secondly, the resistance of the Kresling structures can be modified and controlled according to the magnetic force exerted. Kresling structures with magnetic pieces can be used to form various types of magnetic soft robots.

Significance

The significance of this is to apply the advantages of the magnetic soft materials to actuate Kresling structures: untethered control, fast transformation, broad scale range, and biocompatibility. By using a Kresling origami structure and a magnetic disk as a cell unit, the component can be controlled using a 1D magnetic force. The magnetic disk will rotate due to the torsional forced supplied by the

magnetization, which will cause the component's height to change according to the rotation.

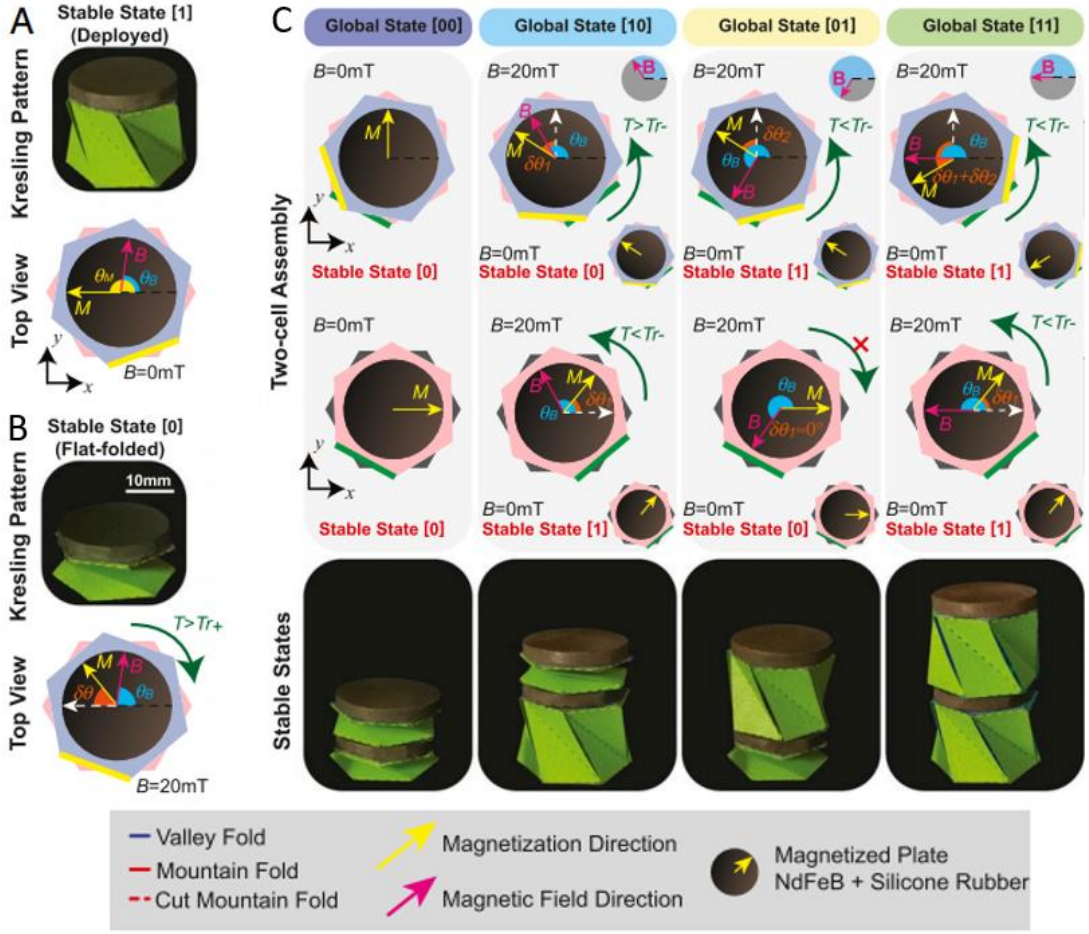

Figure 5. Magnetic actuation of the Kresling pattern and assembly (11). (A) Deployed Kresling pattern and its top view, where θ_B is the direction of the applied magnetic field **B**, θ_M is the direction of the plate magnetization **M**, and $\delta\theta$ is the rotation angle controlled by **B**. (B) Folded Kresling pattern and its top view. (C) Stable states of two-unit Kresling assembly.

Parts A and B of Figure 5 illustrate the idea presented in the above paragraph. Part C in Figure 5 shows that this method can be used on Kresling assemblies. It can be observed that two Kresling assemblies will have four different stable states. In this circumstance, additional deformation can be achieved by adding Kresling unit cells to the assembly.

Motivation for Work

The motivation for this study was based on the biocompatibility characteristics of the magnetic material. As stated above, traditional rigid robotics have limitations, especially in places like human organs. Thus, robots made of soft, biocompatible material can reach areas that rigid robots cannot. With the untethered control, soft robots can be controlled with sources outside human body. Therefore, magnetic soft robotics was studied to contribute to the medical field.

Goal of Research

One of the early goals of this research was to build a three-axis Helmholtz coil that can generate magnetic fields in the x-, y-, and z- directions to control magnetic robotics. The purpose of this device is to control magnetic soft robotics in three different dimensions.

The overall goal in this research was to design and optimize Kresling structures for different magnetic soft robotics applications. When there can be higher magnetic forces applied, the Kresling can have more resistance to stabilize the structures. Similarly, when there is not as much magnetic force actuated, the resistance of the Kresling must be lower.

The research methodology had three main components: the composition of a three-axis Helmholtz coil, drop testing of the Kresling assemblies, and determining how the Kresling designs will be examined. After that, the design and fabrication of different Kresling patterns and the results of the drop tests are illustrated.

Research Methodology

Composition of a 3-Axis Helmholtz Coil

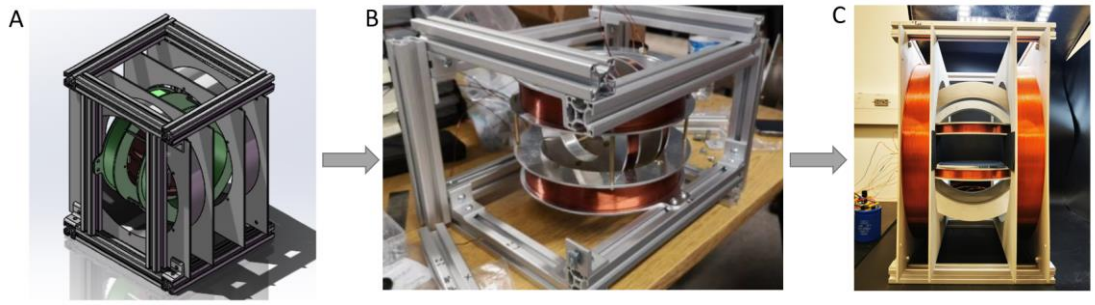

Figure 6. Three-axis Helmholtz coil. (A) SolidWorks model of the Helmholtz coil. (B) Composition process of the coil with only x and y axes. (C) Final product.

The methodology used to create this device involved first measuring whether the overall dimensions and structure were correct. Then the coils were wrapped tightly and precisely. According to part C of Figure 6, the smallest axis is the x-axis in the middle, the second largest coils are along the y-axis, and the largest coils are along the z-axis.

The parameters for this device are as follows:

- X-axis (18 AWG Wire):
  - Inner radius = 50 mm
  - Outer radius = 70 mm
  - Number of turns: 13*18
- Y-axis (18 AWG Wire):
  - Inner radius = 92.5 mm
  - Outer radius = 106 mm
  - Number of turns: 31*12
- Z-axis (17 AWG Wire):
  - Inner radius = 139 mm
  - Outer radius = 151 mm
  - Number of turns: 47*12
- Working Area: 40 mm * 60 mm * 80 mm
- Magnetic field: 30 mT * 30 mT * 30 mT

Drop Test

This method was used to determine the characteristic of the Kresling assemblies composed of four same-sized Kresling bases with different heights. In this test, four Kreslings with differing heights (i.e., $H_1, H_2, H_3, and\ H_4$) were attached to each other one by one. The Kresling with the shortest height was placed on the top, the second-shortest Kresling was attached to the bottom of it, and so of for the third and fourth. They all have a hexagonal base with a side length of 13 mm. The values of $H_1, H_2, H_3, and\ H_4$ are 15.6 mm, 16.9 mm, 18.2 mm, 20.8 mm, respectively. Because there are four Kresling in the assembly, it has $4^2 = 16$ stable states. A small ball was dropped from different heights onto each of the states to see their end states. The stiffness of each state can be obtained.

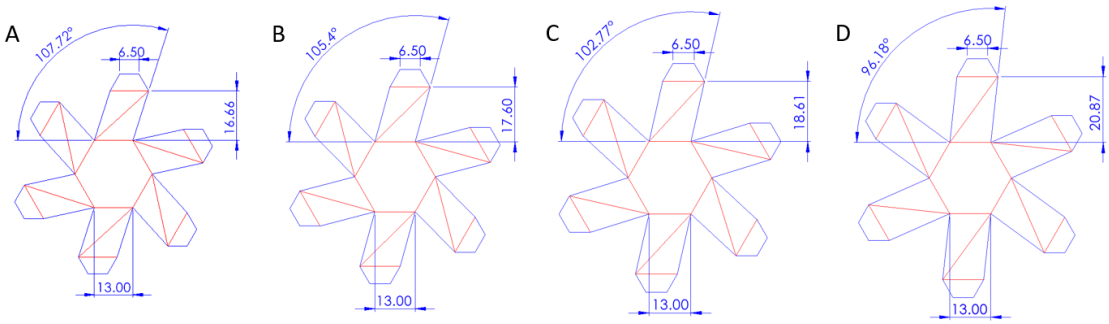

Figure 7. Kresling designs used for drop test. (A) Kresling Design 1 ($H_1 = 15.6\ mm$). (B) Kresling Design 1 ($H_2 = 16.9\ mm$). (C) Kresling Design 3 ($H_3 = 18.2\ mm$). (D) Kresling Design 4 ($H_4 = 20.8\ mm$).

Testing equipment will be created based on the requirements of this test. The stiffness of each global state will be obtained both experimentally and theoretically.

Examination of Different Kresling Designs

This part of the research will be divided into three separate parts for comparison.

1. Modification of the Kresling design shapes: The sizes and shapes of the Kresling bases will be constrained, and the heights will be modified. The resistance will be tested for each design to see how it will be affected by the height change.
2. Modification of the crease design: Vinyl material and a mechanical cutter were used in this part. With the overall shape of the Kresling remaining the same, the resistance of each design will be measured and studied.
3. Modification of the materials: Sheets of different thicknesses and materials like vinyl were used for testing in this circumstance. The design of the Kresling remained the same for all materials for comparison.

Design, Fabrication, & Numerical Results

Design and Fabrication of Kresling Samples

The Kresling structures were designed using SolidWorks and saved as *.dxf* files so they could be read by a laser cutter or mechanical cutter. All the Kresling structures used in this research are hexagon-based. The base side length was set to be 13 mm as the standard size.

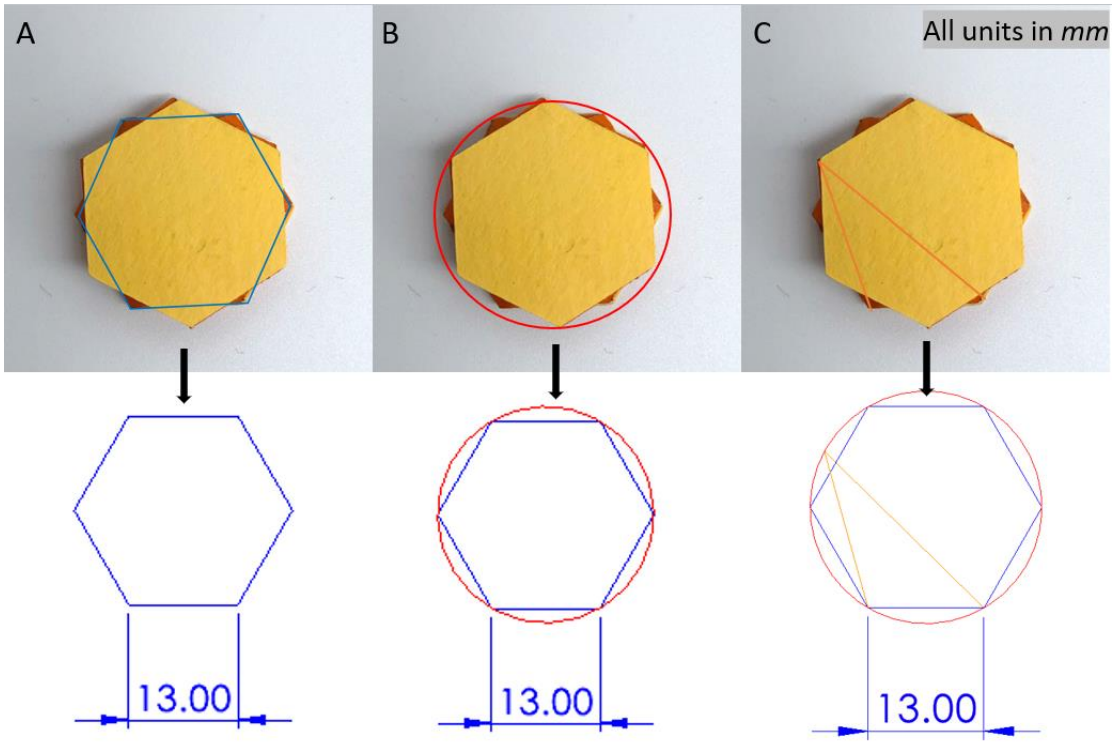

Figure 8. Analysis of folded Kresling in SolidWorks. (A) Top view of a Kresling in its deployed state. The bottom base is outlined with blue. (B) The red line represents the paths that each vertex point goes through during the folding process. (C) The orange line represents the deployed face.

The basic concepts of the folded Kresling pattern are explained in Figure 8. The orange lines form the basic triangular shapes of the Kresling patterns. With the triangle's bottom constrained to 13 mm and the vertex of the triangle moving on the circle, the top angle of the triangle must be 30 degrees (Fig. 9).

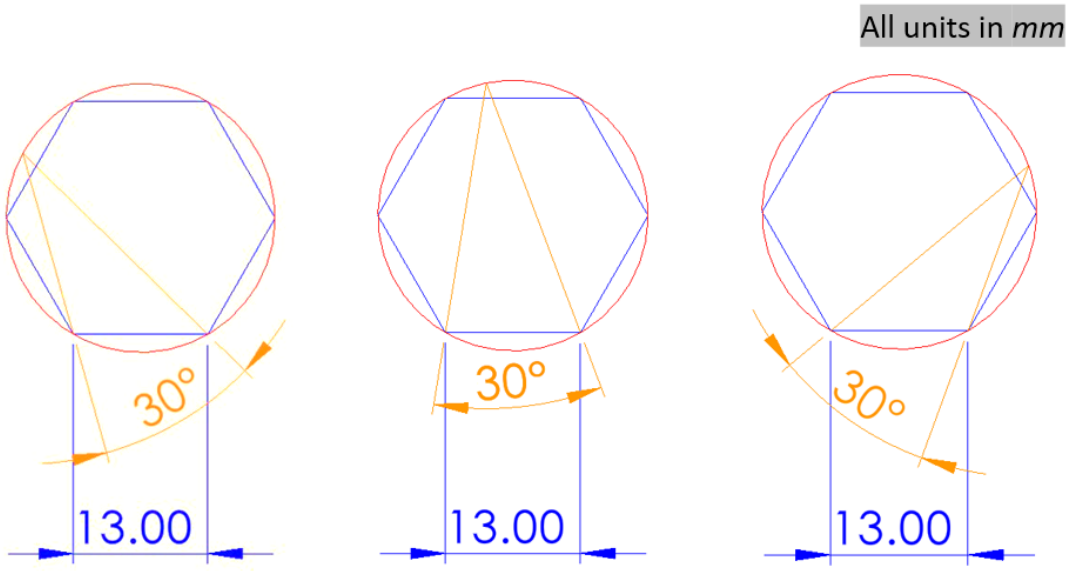

Figure 9. Angle of vertex for different locations

With that being said, the triangle can be fully defined with a defined height. The Kresling structure to be used for fabrication can be created when the lengths of the design are constrained to be equal to the triangle in the circle (Fig. 10).

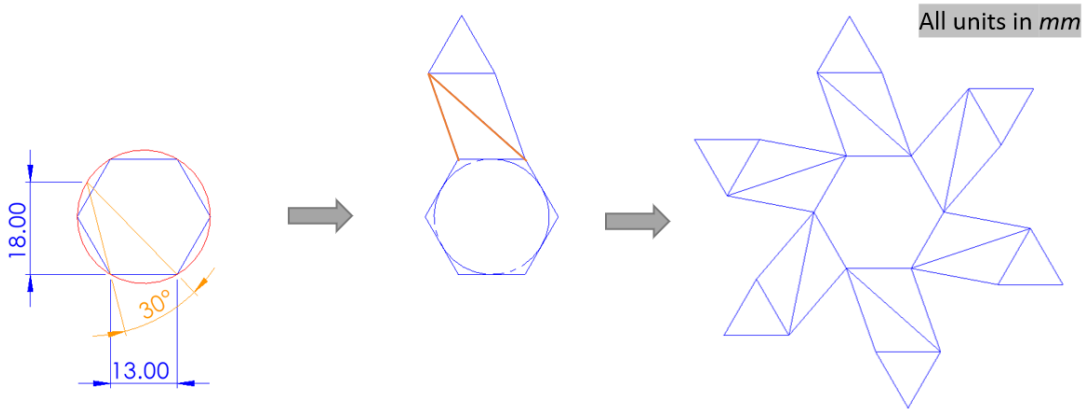

Figure 10. Design of the Kresling structure in SolidWorks (18 mm height)

With the basic structure designed, the fabrication method for the Kresling can be considered. There are two main means of fabrication, using a laser cutter or a mechanical cutter. Although both only read the *.dxf* file, they recognize the files in different ways. The laser cutter can read different layers by color while the

mechanical cutter only read the whole structure as lines to cut. Therefore, the models for the laser cutter have different colors to represent the dashed lines for folding, and the models for the mechanical cutter need to be manually set the dashed lines (Fig. 11).

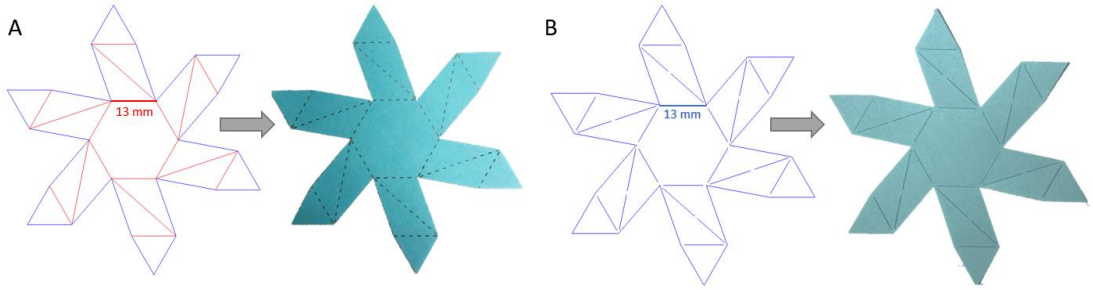

Figure 11. Kresling design difference for different fabrication methods (all heights are 17 mm). (A) Kresling structure for laser cutting fabrication method. The red line represents the dashed lines, and the blue lines are to be cut through. (B) Kresling structure for mechanical cutter fabrication. All lines will be cut through.

With the Kresling structures fabricated, they can be folded and glued to form the Kresling units (Fig. 12). The base material used was thick paper, so it can stay flat during deformation.

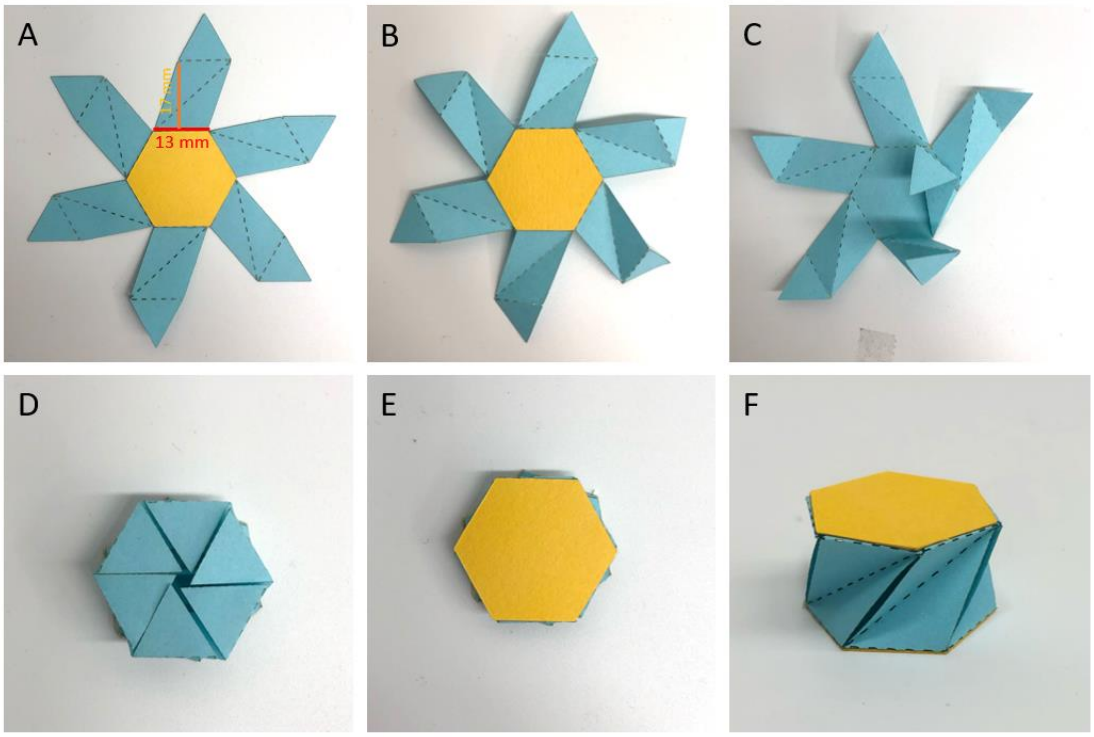

Figure 12. Procedure for folding a Kresling (base: 13 mm, height: 17 mm). (A) Back side of Kresling; (B) Folded with dashed lines; (C–D) Fold; (E) Put on the top base; (F) Completed model.

With the Kreslings fabricated, its characteristics can be studied. To obtain stable and constant results, each Kresling unit cell will be folded 300 times before use.

Drop Test

The drop test started with the design of the testing equipment (Fig. 13A). A ball needs to be dropped from a recordable height, then the dropping height needs to be gradually increased, and the folding stages for the Kresling assembly will be recorded for calculation.

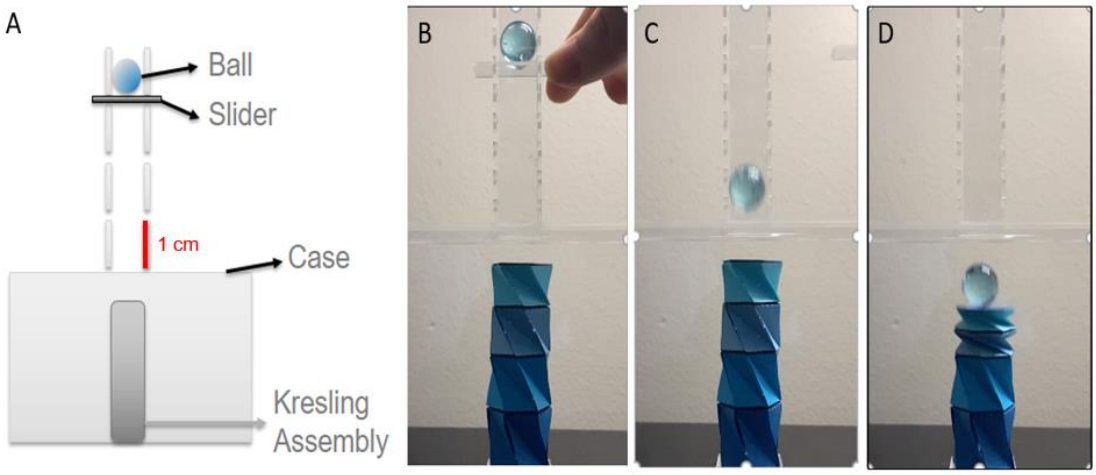

Figure 13. Testing Device. (A) Front of the design of the device (in 2D). (B) Ball starting point. The horizontal bar is pulled slowly to avoid ball rotation. (C) Ball falling. (D) Ball folding top two Kresling units.

The resting device is made of 2-mm-thick acrylic board. The top tube is made to be slightly larger than the size of the ball to constrain the falling point of the ball. The distance between each hole for the slider is 1 cm. In the test, the distance between the ball and the top of the origami was recorded, and the folded Kresling was also recorded. The height of the assembly in different states was also measured and recorded.

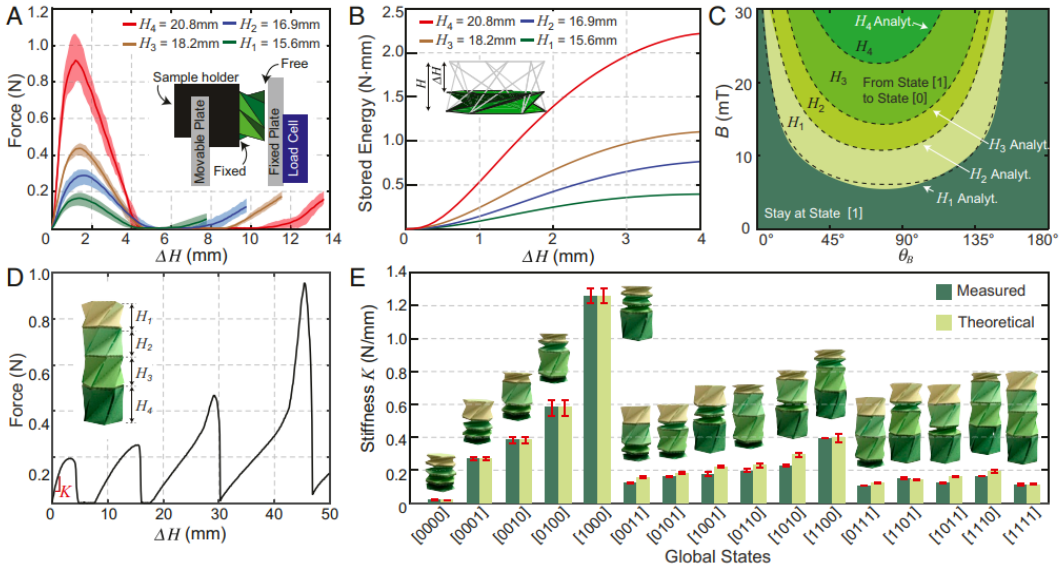

Figure 14. Tunable mechanical response of a multicell Kresling assembly (11). (A) Measured force-displacement curves for unit cells with distinct heights. Solid lines represent the average responses, and shaded envelopes delimit maximum and

minimum response ranges. *Inset* shows the schematic of the compression setup with fixed-free boundary conditions. (B) Stored energy versus axial displacement obtained from the averaged force-displacement curves prior to snapping. (C) Contour plot with measured and analytical (dashed lines) conditions for the magnetic actuation depending on each unit cell geometry. (D) Measured force-displacement curve for a four-cell Kresling assembly in the stable state [1111]. (E) Tunable mechanical response of the four-cell Kresling assembly. From multiple consecutive testing cycles, we obtain the average (columns) and maximum/minimum (error bars) stiffness of the assembly. Theoretical values were approximated using a system of springs in series.

The stable states of the Kresling assembly were named concerning the folded/deployed state of each Kresling unit cell. The number 0 represents the folded state, and the number 1 represents the deployed state. The location of the number represents the Kresling unit cells. It can be observed from Fig. 14 A and B that the compression force and stored energy of the Kresling unit cell will increase when its height is increased. Although the change in height is only about 1 mm for the four designs, their obviously properties vary. The various stiffness levels of the 16 global states are presented in Figure 14 E. The assembly has tunable properties under distributed magnetic actuations.

Mechanical Properties of Kresling

- Varying Heights

The original Kreslings are made of paper. They have energy barriers when folding. The structure snaps. This will cause potential errors and difficulties under distributed controls. Therefore, approaches to mono-stable Kresling structures have been developed. For Kreslings with base side lengths of 13 mm, the mono-state structures are found to have heights of 13 mm or 11 mm.

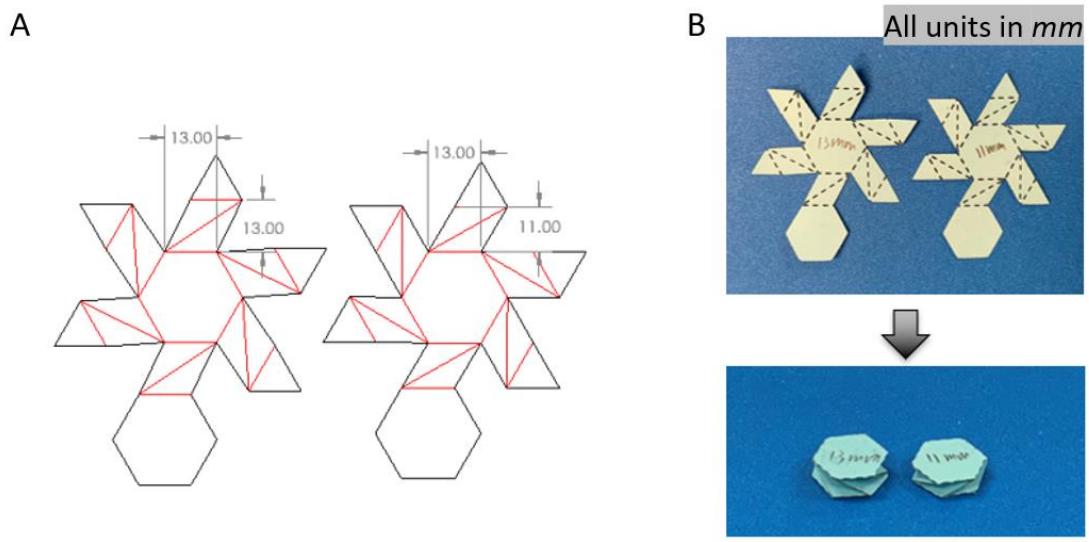

Figure 15. Mono-state approach. (A) SolidWorks models for mono-state Kreslings. (B) Actual models for mono-state Kreslings.

Obviously, the paper mono-state Kreslings are shorter. They cannot provide much vertical deformation when the magnetic field is applied. Also, the resistance of the Kresling greatly increases when the ___ is short. In this case, a soft material called vinyl was used to reduce the resistance of tall Kresling structures. As stated in the previous section, tall Kresling structures will have high levels of stiffness. This also holds true when the material is changed.

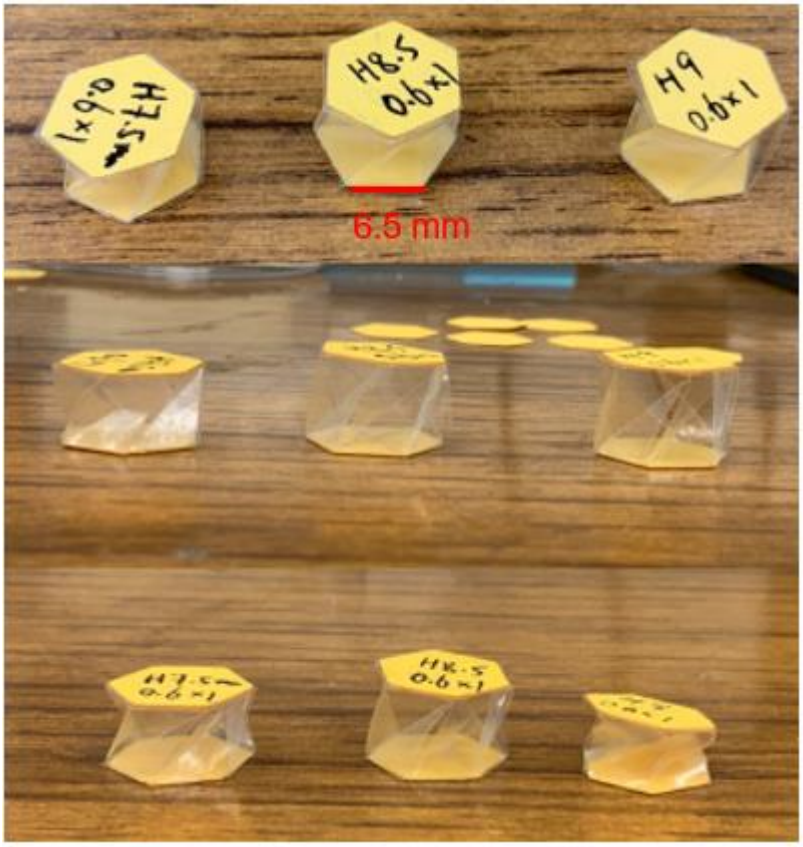

Figure 16. Vinyl Kresling with different heights (50% of original size)

With the soft material, the size of the Kresling structures can be reduced to 50% of its original size. Figure 16 presents three designs of vinyl Kresling structurers with three different heights: 7.5 mm, 8.5 mm, and 9 mm. From the results, it can be observed that the Kresling design with a height of 9 mm is a bi-stable Kresling. Therefore, the height of the mono-state Kresling was increased to be 8.5 mm (17 mm if original size) with this new material. Now, the Kresling structures are taller and have reduced resistance to control.

Different Crease Designs

When the material was changed from paper to vinyl, the fabrication method was

also changed from using a laser cutter to a mechanical cutter. This is due to the fact that lasers can burn vinyl, which will lead to inaccuracy. In this case, the crease design becomes important. With more materials on the crease, there will be increased resistance for the Kreslings. When there are not as many materials used for the crease, the Kresling will not operate as stably as before. Therefore, different crease designs will be adapted for different applications.

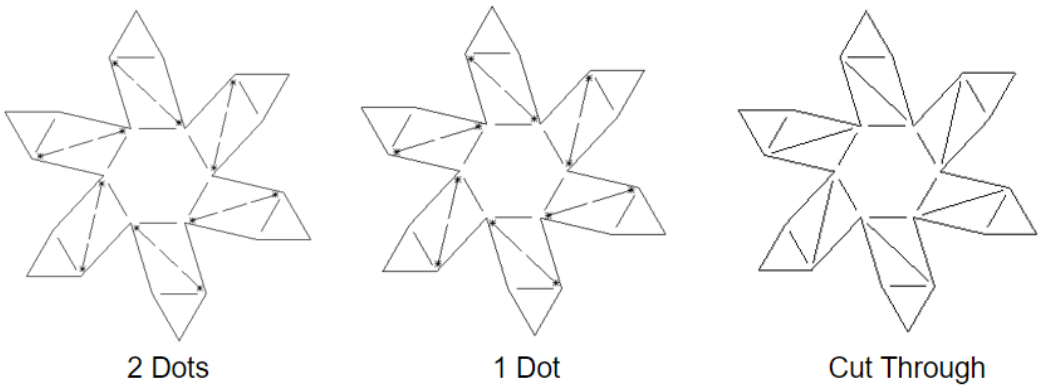

Figure 17. Crease design for mechanical cutter

As stated before, the mechanical cutter is not able to read color and generate dashed lines automatically. Thus, the crease designs were generated manually using SolidWorks drawing. Figure 17 presents three crease designs, the design with two dots in the crease line is used for swimming robots due to its relatively high stability. The design with one dot in the crease line is used for crawling robots due to its relatively low resistance.

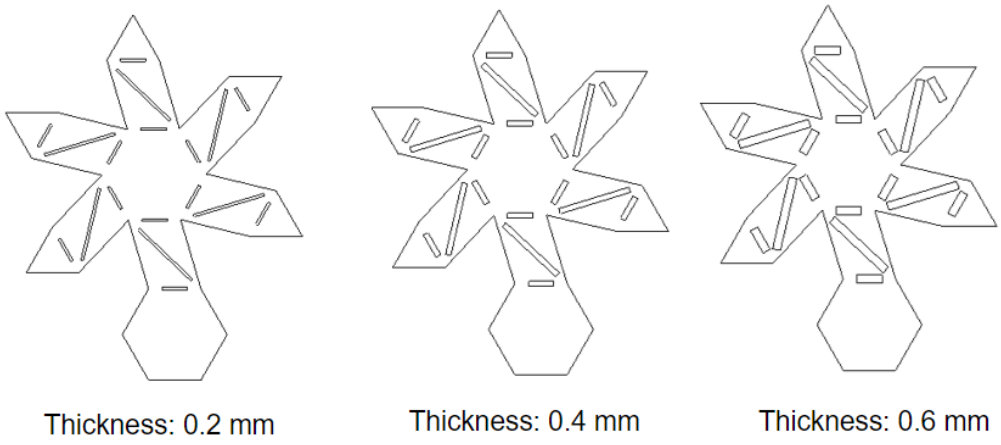

Figure 18. Crease Modification

For bio-medical purposes, Kresling robots need to be reduced in size to fit inside the human body. The crawling robot was reduced to 30% of its original size. However, when the Kresling is reduced, the magnetic disk is also reduced to fit its base. This leads to a reduction in the magnetic force available to control the robot. That is to say, the resistance of the structure must also be further reduced to improve control. Therefore, squares took the place of lines in the designs presented in Figure 18. However, the disadvantage of this design is that it cannot be fold properly.

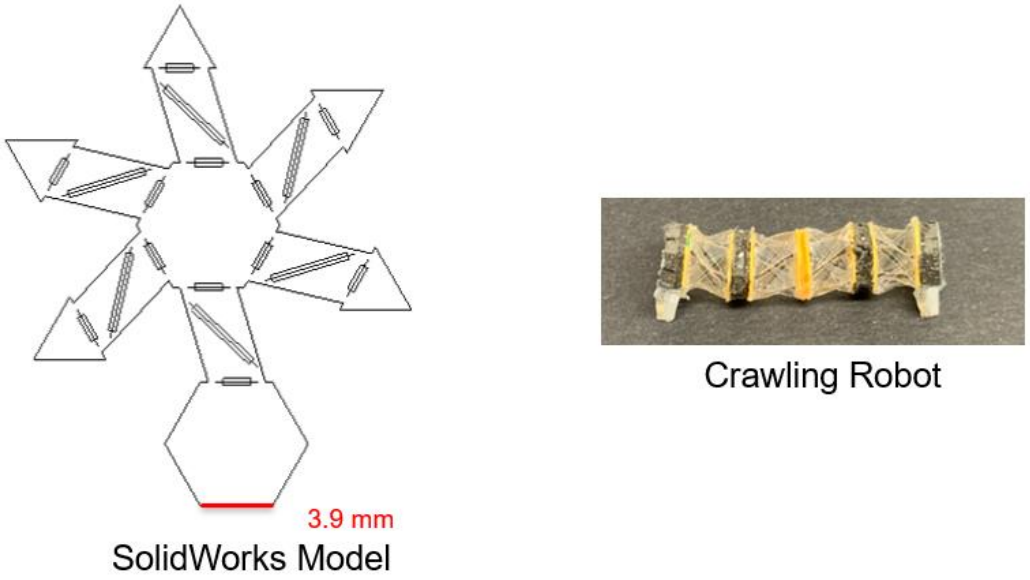

Figure 19. Vinyl Crawling Robot

Thus, the final design of vinyl crawling robot has an added line on the crease to produce the desired shape. With the reduction of the materials on each side, the resistance is also reduced. Therefore, the crawling robot can be created and controlled by using four magnetic disks and two feet. The crawling robot can move to desired locations by properly controlling the magnetic fields.

Different Materials

To further reduce the resistance of the crawling robots, a new material called polyethylene was introduced. This material is softer than the 0.05 mm thick vinyl. With the adoption of this material, the design from Figure 17 with one dot in the crease line can be used for the crawling robots. In this case, the structures produced by a mechanical cutter have a greater accuracy, they are also more similar concerning their properties.

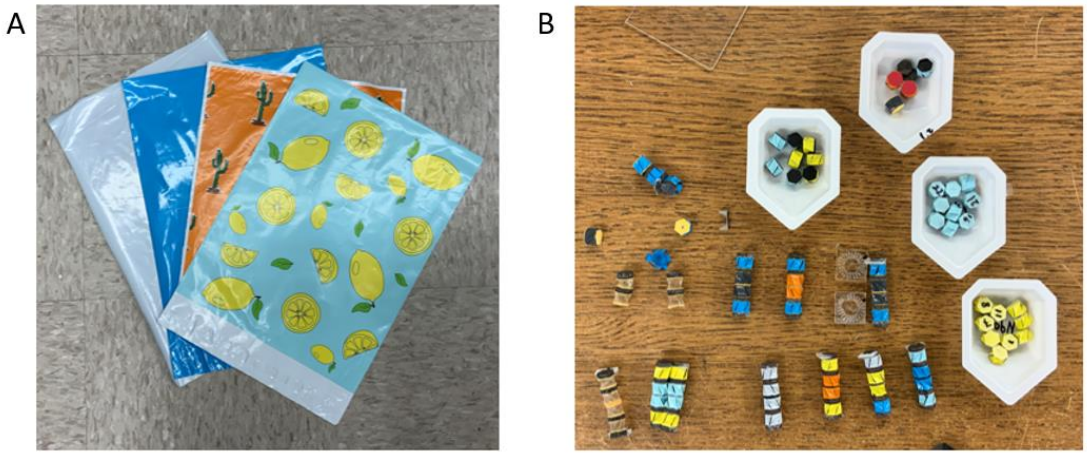

Figure 20. Polyethylene for 30% Kresling robots. (A) Polyethylene. (B) Various polyethylene crawling robots.

With stable properties, the final crawling robot was produced after the compression tests. Each Kresling unit cell was folded 300 times before the compression tests. Then they were labeled with numbers. Their force vs. distance graphs were generated using a compression machine. The Kresling unit cells will be sort into different categories according to the compression forces. The unit cells with the most similar mechanical properties were selected to form the crawling robot.

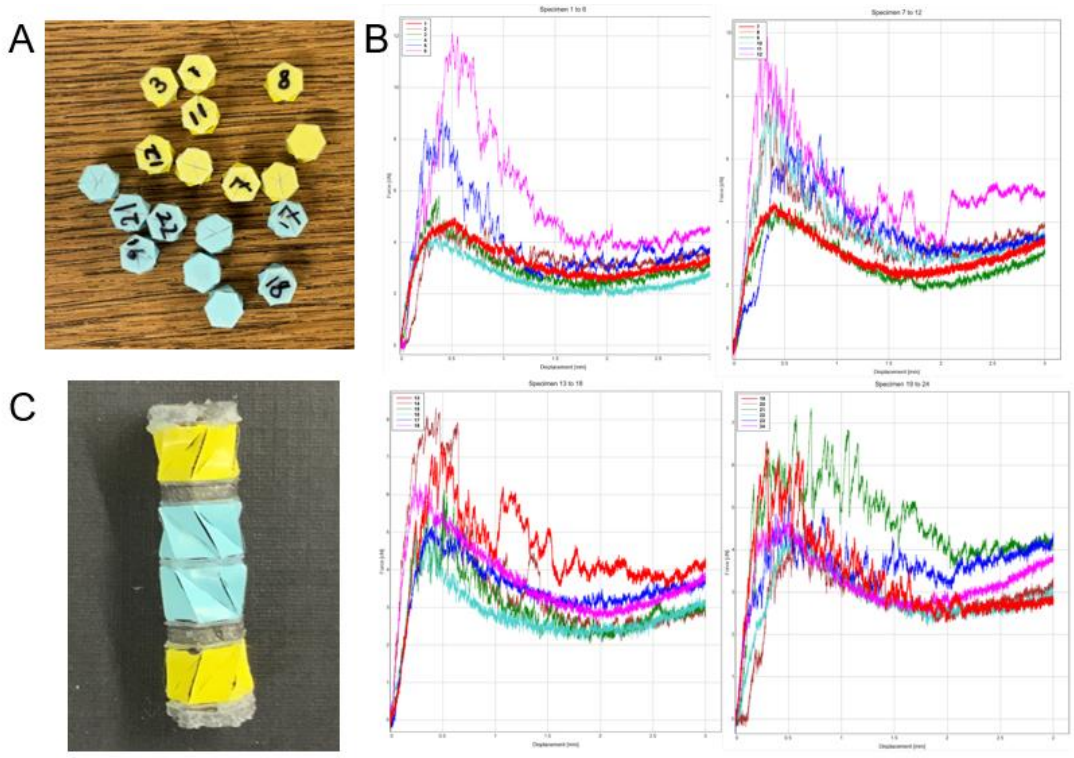

Figure 21. 30% Kresling with compression test results. (A) Numbered Models. (B) Compression test results. (C) Final Crawling robot.

The advantage of this Kresling structure is that it is highly visible during experiments. Also, by having the compression tests, the overall mechanical property of the Kresling assemble will be more uniform. In this case, the robot will be more under control.

Conclusions and Future Work

To sum up everything that has been stated so far, Kresling structures can provide desired deformation when actuated by magnetic soft materials. Kresling assembly properties are also tunable. In this case, the designs can be modified to create Kreslings with different properties for various applications. With softer materials, the Kreslings can be made taller with lower resistances, and the size can be reduced. When fabricated with water-resistant materials, a Kresling can swim in fluid. Combined with the biocompatibility of the magnetic material, increasingly small robots can be created to complete tasks inside human body. The limitations that traditional rigid robots have can be overcome.

However, the study of Kresling structures is not complete. There are many parameters that can be changed in explorations. This may lead to the future study of modified Kresling designs.

Future Work: Modified Kresling Designs

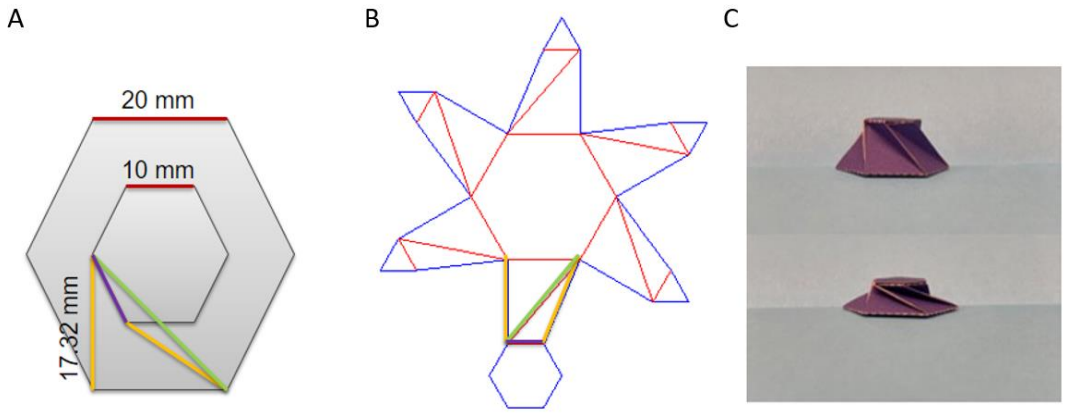

Figure 22. Cone-shaped Kresling. (A) Initial design for folded state. (B) SolidWorks model where the colors indicate lines of the same length. (C) Product in deployed and folded states.

A cone-shaped Kresling can be obtained using a similar approach as in the original design. The top base is set to be half of size of the bottom base, and lines are connected to confirm the crease shapes. This type of Kresling can have different magnetic disks for the top and bottom base. Therefore, the design can have different torsion levels for the top or bottom bases under the same magnetic field.

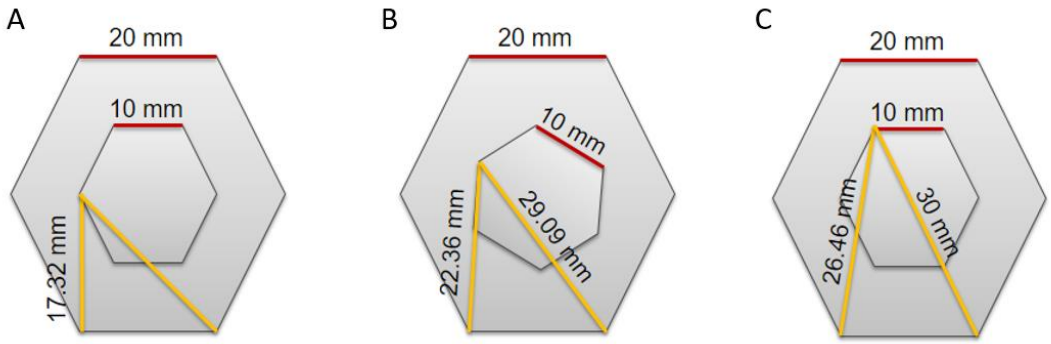

Figure 23. Designs for Cone-Shaped Kresling Structure

Additional models were created according to the initial design. A rotation limitation was also found in Figure 23 C. This limitation is defined to be the maximum rotation of this Kresling when it is folded flat.

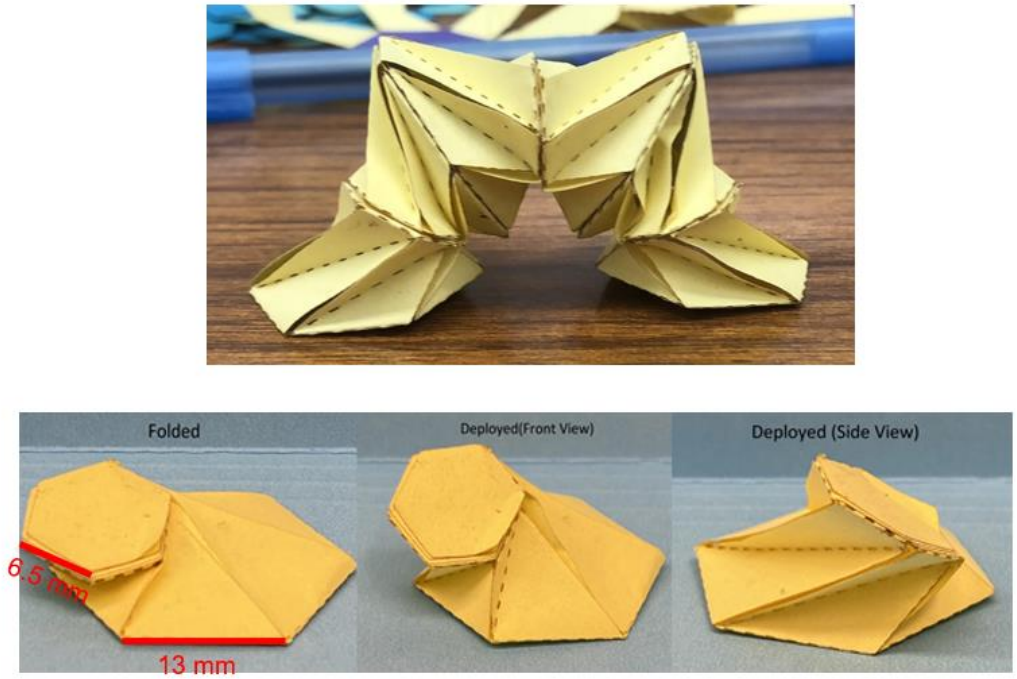

Figure 24. Multi-Shaped Kresling Origami

Structures with tilted deployed states are also considered. This can be easily approached by having the top base not centered on the bottom base. Various structures can be obtained. In this case, the Kreslings are flat when folded and tilted when deployed. The Kreslings will be able to provide deformation in a 3D environment. As presented in Figure 24, when combined with multiple multi-shaped Kresling structures, the structure is able to reach many different directions and angles.

References

[1] Bell, J. (2020, January 03). How four types of medical robots are leading the way in healthcare. Retrieved March 28, 2021, from https://www.ns-healthcare.com/analysis/medical-robots/

[2] Rich, S. I., Wood, R. J., & Majidi, C. (2018). Untethered soft robotics. Nature Electronics, 1(2), 102.

[3] Rus, D., & Tolley, M. T. (2018). Design, fabrication and control of origami robots. Nature Reviews Materials, 3(6), 101.

[4] Wallin, T. J., Pikul, J., & Shepherd, R. F. (2018). 3D printing of soft robotic systems. Nature Reviews Materials, 3(6), 84.

[5] Cianchetti, M., Laschi, C., Menciassi, A., & Dario, P. (2018). Biomedical applications of soft robotics. Nature Reviews Materials, 3(6), 143.

[6] Kim, Y., Yuk, H., Zhao, R., Chester, S. A., & Zhao, X. (2018). Printing ferromagnetic domains for untethered fast-transforming soft materials. Nature, 558(7709), 274.

[7] Wu, S., Ze, Q., Zhang, R., Hu, N., Cheng, Y., Yang, F., & Zhao, R. (2019). Symmetry-Breaking actuation mechanism for soft robotics and Active Metamaterials. ACS Applied Materials & Interfaces, 11(44), 41649–41658. doi:10.1021/acsami.9b13840

[8] Kim, Y., Parada, G. A., Liu, S., & Zhao, X. (2019). Ferromagnetic soft continuum robots. Science Robotics, 4(33), eaax7329.

[9] Ren, Z., Hu, W., Dong, X., & Sitti, M. (2019). Multi-functional soft-bodied jellyfish-like swimming. Nature communications, 10(1), 2703.

[10] Li, Meng & Ostrovsky-Snider, Nicholas & Sitti, Metin & Omenetto, Fiorenzo. (2019). Cutting the Cord: Progress in Untethered Soft Robotics and Actuators. MRS Advances. 4. 1–18. 10.1557/adv.2019.439.

[11] Novelino, L., Ze, Q., Wu, S., Paulino, G. and Zhao, R., 2020. Untethered control of functional origami microrobots with distributed actuation. Proceedings of the National Academy of Sciences, p. 202013292.